Masterclass in Neuroendocrinology Series

Computational Neuroendocrinology

Editors: Duncan J. MacGregor & Gareth Leng

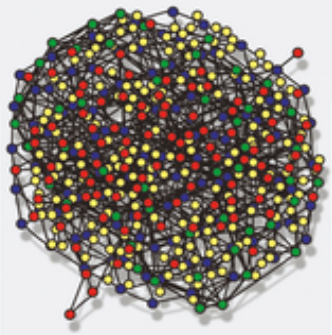

with website

WILEY Blackwell

Computational Neuroendocrinology

Computational Neuroendocrinology

EDITED BY

Duncan J. MacGregor and Gareth Leng

Centre for Integrative Physiology, The University of Edinburgh, UK

WILEY Blackwell

This edition first published 2016 © 2016 by John Wiley & Sons, Ltd

Registered office: John Wiley & Sons, Ltd, The Atrium, Southern Gate, Chichester, West Sussex, PO19 8SQ, UK

Editorial offices: 9600 Garsington Road, Oxford, OX4 2DQ, UK
The Atrium, Southern Gate, Chichester, West Sussex, PO19 8SQ, UK
111 River Street, Hoboken, NJ 07030-5774, USA

For details of our global editorial offices, for customer services and for information about how to apply for permission to reuse the copyright material in this book please see our website at www.wiley.com/wiley-blackwell

Library of Congress Cataloging-in-Publication Data applied for.

ISBN: 9781119951698

A catalogue record for this book is available from the British Library.

Wiley also publishes its books in a variety of electronic formats. Some content that appears in print may not be available in electronic books.

Cover design by Dan Jubb

Set in 9.5/13pt Meridien by SPi Global, Chennai, India

1 2016

Contents

List of Contributors

Richard Bertram
Department of Mathematics and Program in Neuroscience
Florida State University
Tallahassee, FL, USA

Frédérique Clément
INRIA Paris-Rocquencourt Research Centre
Domaine de Voluceau
Le Chesnay, France

Wen Duan
Department of Mathematics
University of Auckland
Auckland, New Zealand

Jianfeng Feng
Department of Computer Science
University of Warwick
UK

Allan Herbison
Department of Physiology
University of Otago
Otago, New Zealand

David J. Hodson
CNRS, Institut de Génomique Fonctionnelle
Montpellier, France
INSERM, Montpellier, France
Universités de Montpellier 1 & 2
Montpellier, France
Department of Medicine
Imperial College London
London, UK

Gareth Leng
Centre for Integrative Physiology
University of Edinburgh
Edinburgh, UK

Stafford L. Lightman
Henry Wellcome Laboratories for Integrative Neuroscience and Endocrinology
University of Bristol
Bristol, UK

Duncan J. MacGregor
Centre for Integrative Physiology
University of Edinburgh
Edinburgh, UK

David P. McCobb
Department of Neurobiology and Behavior
Cornell University
Ithaca, NY, USA

Patrice Mollard
CNRS, Institut de Génomique Fonctionnelle
Montpellier, France
INSERM, Montpellier, France
Universités de Montpellier 1 & 2, Montpellier, France

Francois Molino
CNRS, Institut de Génomique Fonctionnelle
Montpellier, France
INSERM, Montpellier, France
Universités de Montpellier 1 & 2
Montpellier, France
Centre National de la Recherche Scientifique,
Unité Mixte de Recherche
University Montpellier 2
Montpellier, France

Arthur Sherman
Laboratory of Biological Modeling
NIDDK, National Institutes of Health
USA

James Sneyd
Department of Mathematics
University of Auckland
Auckland, New Zealand

Francesca Spiga
Henry Wellcome Laboratories for Integrative
Neuroscience and Endocrinology
University of Bristol
Bristol, UK

Stanko S. Stojilkovic
National Institute of Child Health and Human
Development
National Institutes of Health
Bethesda, MD, USA

Joël Tabak
Department of Mathematics and Program in
Neuroscience
Florida State University
Tallahassee, FL, USA

John R. Terry
College of Engineering
Mathematics and Physical Sciences
University of Exeter
Exeter, UK
Henry Wellcome Laboratories for Integrative
Neuroscience and Endocrinology
University of Bristol
Bristol, UK

Alexandre Vidal
Laboratoire de Mathématiques et Modélisation
d'Évry (LaMME)
Universite´ d'Évry-Val-d'Essonne
Évry, France

Jamie J. Walker
Henry Wellcome Laboratories for Integrative
Neuroscience and Endocrinology
University of Bristol
Bristol, UK

Mary Lou Zeeman
Department of Mathematics
Bowdoin College
Brunswick, ME, USA

Series Preface

This series is a joint venture between the International Neuroendocrine Federation and Wiley-Blackwell. The broad aim of the series is to provide established researchers, trainees, and students with authoritative up-to-date accounts of the present state of knowledge and prospects for the future across a range of topics in the burgeoning field of neuroendocrinology. The series is aimed at a wide audience as neuroendocrinology integrates neuroscience and endocrinology. We define neuroendocrinology as the study of the control of endocrine function by the brain and the actions of hormones on the brain. It encompasses the study of the normal and abnormal functions, and the developmental origins of disease. It includes the study of the neural networks in the brain that regulate and form neuroendocrine systems. It includes the study of behaviors and mental status that are influenced or regulated by hormones. It necessarily includes the understanding and study of peripheral physiological systems that are regulated by neuroendocrine mechanisms.

Clearly, neuroendocrinology embraces many current issues of concern to human health and well-being, but research on these issues necessitates reductionist animal models.

Contemporary research in neuroendocrinology involves the use of a wide range of techniques and technologies, from subcellular to systems and the whole organism level. A particular aim of the series is to provide expert advice and discussion about experimental or study protocols in research in neuroendocrinology and to further advance the field by giving information and advice about novel techniques, technologies and interdisciplinary approaches.

To achieve our aims, each book is based on a particular theme in neuroendocrinology, and for each book, we have recruited an editor, or pair of editors, experts in the field, and they have engaged an international team of experts to contribute chapters in their individual areas of expertise. Their mission was to give an update of knowledge and recent discoveries, to discuss new approaches, "gold-standard" protocols, translational possibilities, and future prospects. Authors were asked to write for a wide audience to minimize references, and to consider the use of video clips and explanatory text boxes; each chapter is peer-reviewed and has a *Glossary*, and each book has a detailed index. We have been guided by an Advisory

Editorial Board. The Masterclass Series is open-ended: books in preparation include *Neuroendocrinology of Neuroendocrine Neurons*, *Neuroendocrinology of Stress*, *Computational Neuroendocrinology*, *Molecular Neuroendocrinology*, and *Neuroendocrinology of Appetite*.

Feedback and suggestions are welcome.

John A Russell, University of Edinburgh, and William E Armstrong, University of Tennessee

Preface

I started wondering about the brain when I was walking up and down the road to school. I was amazed by vision, how we are able to sense light with our eyes and turn it into electrical signals that are somehow reconstructed into conscious experience and the ability to interact with the world. Despite being a teenager, I didn't think much about hormones. I pursued these wonderings by becoming interested in philosophy, and then because I was already into computers, artificial intelligence. In the pre-internet age I gleaned as much as I could mostly from magazine articles, reading of the wonders of neural networks and robotics. The desire to pursue these things was great enough to go and study artificial intelligence and philosophy at university.

How do you pursue the brain? Artificial intelligence teaches you most of all just how difficult all the things that our brains can do are. So marvelous, and potentially powerful that they seem almost impossible, and yet we do them all the time, and the answers to how are in here somewhere. By the end of my first degree, it became clear that if I really wanted answers then I should be a neuroscientist, and an opportunity came along to do modeling in 'neuroendocrinology'. It was a neatly packaged masters (to turn me into a neuroscientist) and a PhD, on exactly the path I wanted to follow, and I didn't worry too much that I didn't know what 'neuroendocrinology' was. When I eventually looked it up I was somewhat disappointed to find out it was hormones. This seemed rather unglamorous besides topics such as vision, motor control, and learning and memory. I had no idea how fortunate I was.

Among neuroscientists, we are remarkably privileged in neuroendocrinology, because we have measurable outputs that we can directly relate to measurable neural activity. And beyond this, we know the purpose of these outputs, how these hormonal signals interact with the body and the greater world. We have access to a complete system to study.

How do we pursue this? First comes the anatomy, discovering the location and physical nature of the elements involved in the system. Then the physiology, measuring these elements, detecting their activity, and relating this to function. The hard-won knowledge comes in many small pieces and at many levels, higher level measurements such as hormone concentration in blood plasma, and lower levels such as changes in mRNA content in some component of a cell. Occasionally, these results are easily built into

a more complete understanding of how the systems work, but more often there are large gaps and apparent contradictions. We are also not good at combining knowledge from different levels. A common mistake in neuroscience is the attempt to interpret any result directly in the context of high level system behavior. Every experiment and result must be justified by purpose, and given context, but we often struggle to build the structures to do this, and fall back on lazy reductionism.

What we need are the tools to structure our knowledge and to ask better questions. Many of us have a model of some sort in our heads, written as a hypothesis, or drawn as diagram, but with the skills to formalize these models, and turn them into testable living things, they can be much more powerful. Building models also brings discipline, forcing us to consider what we know and don't know, and most importantly what we *need* to know. In an ideal modelers' world every piece of work would be centered on building a model. The model would be used to plan experiments, interpret results, and ultimately, demonstrate and document the working understanding of a system, as the final product of the research.

The basic skill required for modeling is to be able to translate physiological mechanisms into a mathematical form. There are many well-established techniques for doing this. Mostly they use very simple high-school-level mathematics. More complex analysis is often applied, but this is not necessary to do useful modeling. One basic form is the Hill equation. This models the activation of some element due to binding of a ligand to a receptor. It has two parameters, one for threshold, and one for gradient, and generates a *sigmoid* curve, of the familiar form often seen in dose-response data. Another classic and very successful technique, which features in several chapters of this book, is the Hodgkin–Huxley model. It represents the currents that sum together to generate a neuron's membrane potential. It is able to very accurately reproduce electrophysiological data, bridging our knowledge at the level of individual ion channels and their mechanisms to action potentials and all their variations in shape and patterning. It is successful because both its low-level elements and parameters, and its high-level output can be directly compared to experimental data.

The detail we include in a model will be determined partly by the knowledge we have from which to build it, but also at what level we hope to understand a system, and what data we will test the model against. A guiding principle is that the model should be as simple as possible in order to explain the observed behavior. The Hodgkin–Huxley model is powerful, but it is more difficult to apply to neurons studied *in vivo* where we have less direct access to detailed electrophysiological properties. The alternative is integrate-and-fire type models of action potential generation, where more simple equations with fewer parameters reduce the complex changes

in membrane potential to just the essential changes in neuronal excitability. The more complex models help us to know what elements should be in the simpler model, but we can simplify these elements so that they are easier to work with, and easier to interpret in the context of the behavior of the model.

When we want to study an entire system, such as the HPA axis or the activity of GnRH neurons in the context of an ovarian cycle, we will use a much more abstract representation. A single variable in the model might represent the activity and secretory output of an entire population of neurons. We can use such models to understand how the major elements of the system must interact in order for the system to function and explain the behavior we observe, such as pulsatile hormone output. We will only add more complexity to the model when we determine that more elements are necessary to its functioning. Sometimes these new elements will be based on mechanisms we already know, and sometimes they will be entirely new predictions, to test experimentally.

The objective of this book is to make these techniques accessible to interested experimental neuroendocrinologists and other neuroscientists, and perhaps also to draw those already with the skills for modeling into neuroendocrinology, because hormones are glamorous! All the essential and wonderful elements of life depend on hormones. And as a general way to pursue intelligence and the brain, neuroendocrinology gives us one of the best paths to be able to understand neurons (and glia) and how they process information to drive function.

Our authors are some of the very best in the field of computational neuroendocrinology. They come from diverse backgrounds: mathematics, computing, biology, and medicine, and many of them do both theoretical and experimental work. All of the chapters present examples where modeling has been successfully applied; however, they also tell the story of how they got there, and will hopefully show experimentalists how they can think like modelers, with a view to making use of models and even developing their own.

About the Companion Website

This book is accompanied by a companion website:

www.wiley.com/go/leng/computational

The website includes:

- PowerPoint figures and PDF tables from the book
- A glossary of keywords
- Videos and data sets

CHAPTER 1

Bridging Between Experiments and Equations: A Tutorial on Modeling Excitability

David P. McCobb[1] *and Mary Lou Zeeman*[2]

[1]Department of Neurobiology and Behavior, Cornell University, Ithaca, NY, USA
[2]Department of Mathematics, Bowdoin College, Brunswick, ME, USA

The goal of this chapter is to empower collaboration across the disciplines. It is aimed at mathematical scientists who want to better understand neural excitability and experimentalists who want to better understand mathematical modeling and analysis. None of us need to be expert in both disciplines, but each side needs to learn the other's language before our conversations can spark the exciting new collaborations that enrich both disciplines. Learning is an active process:

> *Tell me and I will forget; show me and I may remember; involve me and I will understand.*
>
> –Proverb

We have, therefore, written this chapter to be highly interactive. It is based on the classic model of excitability developed by Morris and Lecar (1981), and built around exercises that introduce the freely available dynamical systems software, XPP (Ermentrout, 2012), to explore and illustrate the modeling concepts. An online graphing calculator, such as Desmos (www.desmos.com), is also used occasionally. The modeling and dynamical systems techniques we develop are extremely versatile, with broad applicability throughout the sciences and social sciences. In the chapters of this volume, they are applied to systems at scales ranging from individual cells to entire neuroendocrine axes. We recommend that you work on the exercises as you read, with plenty of time, and tea and chocolate in hand. It is a great way to learn.

Outline. In Section 1.1, we introduce excitability, encompassing the diversity of action potential waveforms and patterns, recurrent firing, and bursting. We also describe the voltage clamp, the essential tool for dissection of excitability used by Hodgkin and Huxley (1952)

Computational Neuroendocrinology, First Edition. Edited by Duncan J. MacGregor and Gareth Leng.

Companion Website: www.wiley.com/go/Leng/Computational

in their foundational work. In Section 1.2, we introduce the classic, two-dimensional Morris–Lecar model, developed originally from barnacle muscle data to expose the minimal mathematical essence of excitability (Morris and Lecar, 1981). In Sections 1.3 and 1.4, we introduce the software package XPP (see Section 1.3 and Ermentrout (2012)) for download instructions), and use it to explore the model behavior, thereby introducing the language and graphics of dynamical systems and phase-plane analysis. This provides a platform for extending the model and including data from naturally occurring ion channels to dissect the excitability of diverse and more complex cells.

In Sections 1.5–1.10, we follow the seminal paper by Rinzel and Ermentrout (1989) to explore the surprising richness of behavior the Morris–Lecar model can exhibit in response to sustained current injection at various levels. We use three different parameter sets, differing only in the voltage dependence and kinetics of potassium channel gating. For each parameter set, we simulate a current clamp experiment in which sustained current is applied to a cell at rest. In all the three cases, sufficiently high levels of applied current induce tonic spiking, but the onset of spiking occurs through different mechanisms with different properties. With the first parameter set ("Hopf" in Table 1.1), tonic spiking is restricted to a narrow frequency range, as in Hodgkin's Class II, typically resonator, neurons (Hodgkin, 1948). The second parameter set ("SNIC" in Table 1.1) exhibits tonic spiking with arbitrarily low frequency, depending on the applied current, as in Hodgkin's Class I, typically integrator, neurons. The final parameter set ("Homoclinic" in Table 1.1) generates tonic spiking with a high baseline between the spikes. In Section 1.10, we exploit the high baseline to illustrate how adding a slow variable to the model can generate bursting behavior. Our tour of the Morris–Lecar model owes much to Rinzel and Ermentrout (1989) and many others, including Ellner and Guckenheimer (2006), Izhikevich (2007), Morris and Lecar (1981), and Sherman (2011).

Mathematically, a qualitative change in system behavior, such as the onset of spiking arises through a bifurcation. Different mechanisms for the onset of spiking correspond to different bifurcations. We work through each of these bifurcations carefully, as they typify the mechanisms for generating oscillations in two-dimensional systems, they can underlie mechanisms in higher dimensional systems, and they recur throughout the text.

Our interdisciplinary conversations have led to a route through the mathematical material that may seem unusual. We have not begun with local linear stability theory, because our experience suggests that, while many experimentalists have excellent intuition about rates of change at their fingertips, the abstraction of eigenvalues presents a road block. (This is a natural consequence of the typical mathematics requirements for a

biology degree.) We have chosen, instead, to harness the intuition about rates, and the visual intuition afforded by XPP, to develop an insight into the global nonlinear dynamics and bifurcations of the system. Only then we conclude with a discussion of the role eigenvalues play in determining local stability, and thereby signalling bifurcations. References are provided for the interested reader to learn more.

1.1 Introducing excitability

Action potentials: Decisive action and "information transportation". Cellular excitability is defined as the ability to generate an action potential (or spike): an explosive excursion in a cell's membrane potential (Figure 1.1). Its all-or-nothing aspect makes it decisive. Its propensity to propagate in space enables signal transmission in biological "wires" that are too small and electrically leaky to transmit a passive electrical signal over more than a millimeter or 2. Most cells have strong ionic gradients that are nearly, but imperfectly counterbalanced: a higher concentration of potassium ions (K^+) inside than out, versus higher sodium (Na^+), calcium (Ca^{++}) and chloride (Cl^-) concentrations outside than in. Higher "resting" permeabilities of the cell membrane to K and Cl result in a significant inside-negative *resting potential* (for largely historical reasons this is referred to as a *hyperpolarized* state). Action potentials are explosive excursions in the positive (*depolarizing*) direction from the resting potential, often reversing the polarity substantially (but still referred to as depolarizing).

The explosive mechanism uses positive feedback to produce a spatially regenerative event that propagates along a nerve axon, muscle fiber, or secretory cell's membrane. Positive feedback arises from the fact that the opening of either sodium (Na) or calcium (Ca) ion channels (small selective and gated pores in the cell membrane) is (1) promoted by depolarization and (2) leads to further depolarization, as Na or Ca ions enter through the opened channels. The explosive depolarization can propagate at rates anywhere from 1 to 200 m/s (Xu and Terakawa, 1999) depending on cell specifics. This is very slow compared to the passive spread of a voltage signal in a metal wire (on the order of the speed of light!). It is limited by the time required for channels to respond to voltage, together with the effects of membrane capacitance and leak. Nevertheless, it is much faster than any other form of chemical or biochemical signal propagation, and fast enough to support animal life, including the transmission of information over some 2 million miles of axons in the human body.

The explosive, roughly all-or-nothing nature of the action potential also serves as a decisively thresholded regulator of Ca entry. It thereby regulates many precisely timed and scaled cellular events, including

neurotransmitter and hormone secretion, muscle contraction, biochemical reactions, and even gene regulatory processes. Membrane voltage thus underlies rapid signal integration in the "biological computer," including the regulation of neuroendocrine function.

For a cell to recover from the excursion from negative resting potential and prepare to fire another action potential, repolarization has to occur. This is achieved by combatting the positive feedback with slightly delayed negative feedback, or feedbacks. An essentially identical mechanism of depolarization-triggered opening of ion channels as described for Na or Ca, but now involving a channel type that selectively conducts K, quickly restores the hyperpolarized state. In response, the Na- or Ca-channel gates can now relax back to the closed state (as do the K-channel gates), a process referred to as *deactivation*. In most cases, the K-channel restorative mechanism is backed up by the closing of a separate *inactivation* gate within the body of the Na or Ca channel, which would prevent prolonged depolarization (and flooding of Na or Ca into the cell) even without the K channel. Together these events speed repolarization, deactivation and *deinactivation* (the reversal of inactivation). The separability of these gating events provides raw material for very sophisticated and sometimes subtle differences in firing and consequent signal integration.

Action potential shape and timing in information processing. Synaptic transmission is well known to play important roles in information processing. The details of intrinsic excitability of neuroendocrine cells are at least as important as in neurons, and even more so in cells like those in the anterior pituitary that are not directly driven by synaptic inputs. Thus, the variety, subtlety and susceptibility to modulatory changes of ion channels underlying excitability are critical to the nuances of neuroendocrine signalling. See Hille (2001), Chapter 7 in Izhikevich (2007) and Figure 1.1. Details of the rising phase control threshold and rise time, and influence frequency. The details of repolarization, recovery, and preparation for subsequent signalling events are even more nuanced and diverse, as indicated by the enormous diversity of K channels (at least an order of magnitude greater than that of Na and Ca channels). Action potential threshold, differing between cells, and depending on recent events and modulatory factors within a cell, determines whether a response is transmitted or squelched. It also contributes, as do ensuing features of the action potential, to the encoding of the stimulus strength as firing frequency. Spike amplitude shapes calcium channel activation and calcium entry, as well as K-channel activation. These in turn sculpt ensuing features, and, especially through calcium influx, sculpt the transduction from electrical response to output, including, for example, transmitter, modulator, hormone release, or muscle contraction. The latency of the rising phase is critical to encoding or integration, and can serve as a temporal filter. So, too, can the timing of repolarization

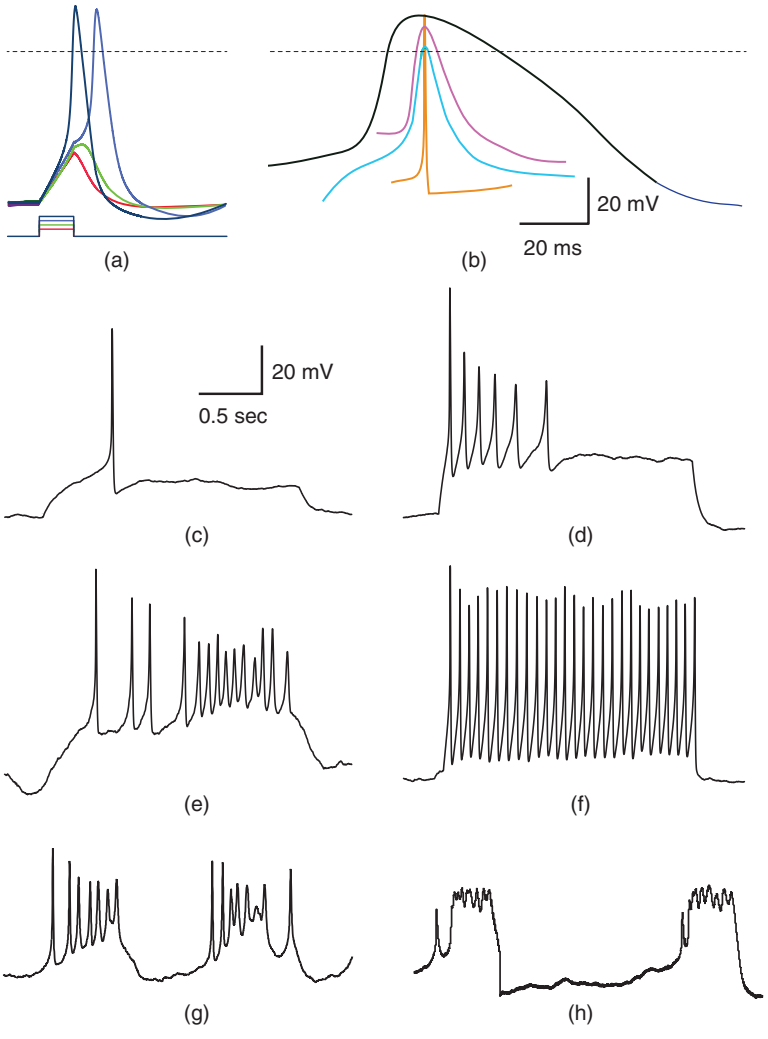

Figure 1.1 Variety of natural excitability. (a) Voltage responses of a mouse adrenal chromaffin cell to 10 ms current steps, recorded with whole-cell current clamp (McCobb Lab data). Action potential (AP) amplitudes were nearly invariant, and rise times varied modestly with stimulus amplitude. Voltage scale as in (b). (b) AP waveforms vary widely between cell types, ranging in duration from 180 μs for a purkinje cell (orange; Bean (2007)) to > 80 ms for a cardiac muscle AP (black). Shown for comparison are spikes from a barnacle muscle cell (blue; Fatt and Katz (1953)) and a chromaffin cell (purple; McCobb Lab). (c–f) Patterns of spikes elicited with sustained current steps vary even between mouse chromaffin cells (McCobb Lab). Cell (c) would not fire more than one spike, (d) fired a train with declining frequency, amplitude, and repolarization rate, (e), an irregular volley, and (f), a very regular train at high frequency. (g, h) Pituitary corticotropes fire spontaneous bursts with features that vary between bursts and between cells, including spike amplitudes and patterns, as well as burst durations (McCobb Lab). Scale bars in (c) apply to (c–h).

and recovery. These can confer a resonance on the system that makes it selectively responsive to timing of input, and potentially, as responsive to hyperpolarizing as depolarizing input. Timing and the interplay between the channel mechanisms together pattern the timing of spikes. They can also confer intrinsic firing, exemplified by the beautifully complex rhythms of burst firing. In addition to influencing reactivity to inputs, intrinsic firing makes a neuron a potential source of action (or maintenance or inaction). Together the dimensions of complexity and variability that have evolved in electrical signalling contribute enormously to the intelligence of biological systems, including (but not exclusive to) the brain function.

Dissecting action potential mechanisms with voltage clamp. Hodgkin and Huxley (1952) used the *voltage clamp* to dissect the action potential in the squid giant axon. (The axon is a milimeter or more in diameter, roughly 100 times the diameter of the largest human fibers). This clever device measures the opening and closing of ion channels, as follows: the voltage difference between the inside and outside of an axon is measured, and compared to a desired or "command" voltage. Any discrepancy between measured and command potentials is then immediately eliminated by injecting current into the axon through a second internal electrode. The amount of current required to clamp the voltage depends on the membrane conductance (inverse of resistance), and thus changes as ion channels open or close (see Figure 1.2). While useful for studying any channels, the voltage clamp is especially important for voltage-gated channels. By varying the voltage itself in stepwise fashion, Hodgkin and Huxley were able to prove that the membrane had conductances that were directly gated by voltage. Then by removing Na and K ions independently, they resolved distinct inward and outward components, and noted their dramatically different kinetics. The inward (Na) current responded more rapidly, but terminated quickly, while the outward (K) current was slower but persisted. Recognizing that this voltage sensitivity might provide the feedback underlying the action potential, they carefully measured voltage- and time-dependent features, including activation and deactivation of inward and outward components, and inactivation and deinactivation of the inward component. They then constructed a mathematical model and solved it numerically for the response to a stimulus, with the similarity between the theoretical voltage response and a recorded action potential supporting the view that they had explained the basic mechanism.

So why do we need to continue modeling action potentials and excitability? Hodgkin and Huxley (1952) predated the identification of ion channel proteins,

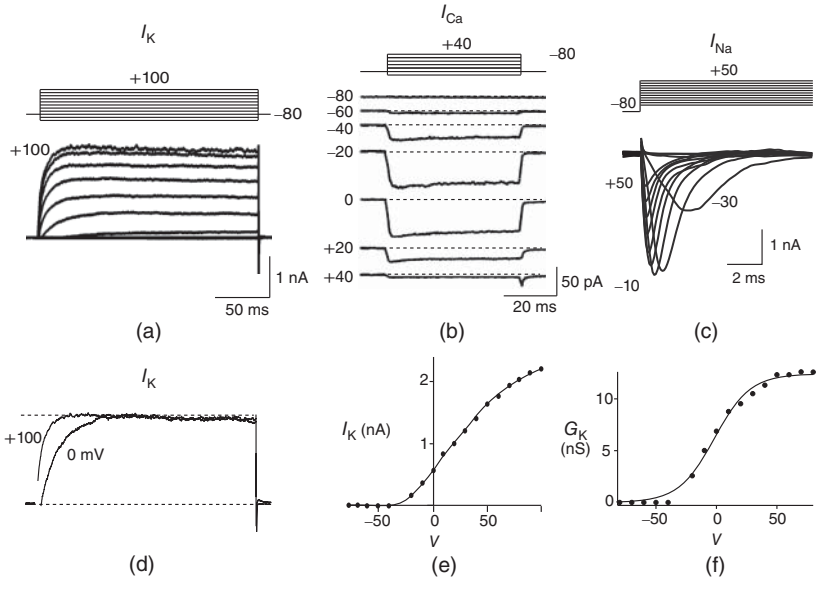

Figure 1.2 Voltage clamp data. (a, b, and c) Voltage-gated K, Ca, and Na currents, respectively, elicited with voltage steps in whole-cell voltage clamp mode applied to mouse chromaffin cells (McCobb Lab data). Outward currents are positive (upward), and inward currents are negative (downward). The K and Ca currents shown here exhibit little inactivation, though both types can inactivate in some chromaffin cells. The Na currents inactivate rapidly, and the current amplitude reverses sign when the test potential crosses the Na reversal potential. (d) K-current activation is faster at more depolarized potentials, as shown by normalizing the K currents at 0 and +100 mV from (a). (e) Current–voltage (*I–V*) plot for K currents from the cell in (a); peak current values are plotted against the corresponding test potential. (f) Conductance–voltage (*G–V*) plot; current values from (e) are divided by the driving force ($V_{test} - V_{reversal}$) and plotted against test potential. The *G–V* curve gives a summary of the voltage dependence of gating without the confounding effect of driving force.

but their results implied sophisticated voltage-sensing and gating nuances, and gave birth to structure-function analysis with unprecedented temporal resolution. Action potentials in barnacle muscle, another early preparation, were shown to depend on Ca rather than on Na influx (Keynes *et al.*, 1973). This laid the foundation for the Morris–Lecar model, in which one (excitatory) Ca current and one (repolarizing) K current interact to generate excitability (Morris and Lecar, 1981). Moreover, with glass electrodes enabling recordings in many more cell types, it became ever clearer that there was enormous variation on the general theme, begging further dissection. Every quantifiable feature of action potentials, from threshold to rise-time, duration, ensuing dip (*afterhyperpolarization*) and size, number, frequency, and pattern of additional action potentials elicited

by various stimuli could be shown to vary from cell to cell. It is now clear that this variety sculpts signal input–output relationships for neurons and networks in almost limitless fashion. Meanwhile, a vast array of ion channel genes, accessory proteins, and modulatory mechanisms contributing to excitability has been identified (Coetzee *et al.*, 1999; Dolphin, 2009; Hille, 2001; Jan and Jan, 2012; Jegla *et al.*, 2009; Lipscombe *et al.*, 2013; Zakon, 2012). A wealth of questions arise. How do structural elements and combinations encode functional nuances appropriate to physiological, behavioral, and ecological contexts in diverse animals? How did they arise through evolution? How they are coordinated in development? And how does event-sensitive plasticity contribute to adaptive modification of excitability-dependent computations? Relevant hypotheses clearly depend on theoretical dissection via mathematical modeling.

Why work with a model originating in barnacle muscle? Throughout the chapter, we will work with the Morris–Lecar model, which was originally developed for barnacle muscle and includes only two voltage-gated channel types (Ca and K), neither of which inactivates. Moreover, based on observations that showed the activation rate for the excitatory Ca current to be about 10-fold faster than that for the repolarizing K current and 20-fold faster than that for charging the capacitor (Keynes *et al.*, 1973), Morris and Lecar (1981) simplified the model even further, reducing dimension by treating the Ca-channel activation as instantaneous.

You may ask why a neurobiologist or endocrinologist should spend time on such a simple system, so obviously peripheral to sophisticated neural computation. Or how simplification and omission justify the trouble of learning mathematical "hieroglyphics". These questions raise the issue of what a mathematical model is good for. A powerful use of models is to help test hypotheses and design experiments about putative biological mechanisms underlying observed behaviors. To that end, minimal models, built from the ground up, allow for thorough dissection and attribution of mechanisms. For example, see Izhikevich (2007, Chapter 5) for a summary of six minimal models of excitability. After studying the Morris–Lecar model in this chapter, we hope that you will agree that what may at first look like an extremely limited system turns out to be capable of a surprisingly rich repertoire of waveforms and firing dynamics. Without studying such a minimal model, one might assume that more channel types or more complex gating mechanisms were needed to generate such a variety. After developing modeling confidence, it is easy to adjust parameters, or add inactivation, other channel types or gating mechanisms, as detailed in Chapter 2. The comparison between Morris–Lecar, Hodgkin–Huxley, and other model

behaviors then helps to clarify the interactive mechanisms at play, and the roles of specific terms and parameters.

The reduced dimension of the Morris–Lecar model also provides an excellent starting point for model analysis. It allows us to explore and dissect the model behavior in a two-dimensional *phase plane* (detailed in Section 1.4), where, with the help of graphical software, we can harness our visual intuition to understand the concepts and language of dynamical systems. The dynamical systems approach is extremely versatile, generalizing to more complex models and higher dimensions, and highlighting similarities among mechanisms in a wide range of applications. Throughout this volume, we will see how dynamical analysis of minimal models, designed with the scale and complexity of the specific neuroendocrine question in mind, yields new biological insights.

1.2 Introducing the Morris–Lecar model

The Morris–Lecar model is discussed in many texts in mathematical biology and theoretical neuroscience. See, for example, Ellner and Guckenheimer (2006), Ermentrout and Terman (2010), Fall *et al.* (2005), Izhikevich (2007), and Koch (1999).

What is in the Morris–Lecar model? The model structure is represented by the circuit diagram in Figure 1.3a (Morris and Lecar, 1981). A system of Ca and K gradients with selective conductances provides "batteries" defining equilibrium or reversal potentials. There is also a "leak" of undefined (probably composite) conductance, with a measurable reversal potential. For our purposes, the chemical gradients do not change appreciably: ion pumps and exchangers work in the background to ensure this. Currents applied through the current electrode travel in parallel across the capacitor and any open ion channels or other leaks. Internal and external solutions offer no resistance to flow, so that the voltage across the capacitor and resistors/conductors in the membrane is equivalent. Moreover, the system is assumed to be spatially uniform; voltage over the entire membrane changes in unison. This fits well with data from compact neuroendocrine cells (Bertram *et al.*, 2014; Liang *et al.*, 2011; Lovell *et al.*, 2004; Stojilkovic *et al.*, 2010; Tian and Shipston, 2000). The approach is also useful for membrane patches in most neuronal contexts. Spatial nonuniformity and spatio-temporal propagation of signals are not addressed here.

What makes this an "excitable" membrane and an interesting dynamical system, is (1) feedback: the proportion of channels open (for both Ca and K channels) depends on voltage and (2) reactions of the channel gates

to changes in voltage take time. Reaction rates also vary with voltage; but while this influences the voltage waveform, it is not essential for excitability.

Ion channel openings and closings are stochastic events, but their numbers are large enough that the currents associated with each type can be modeled as smooth functions. Thus, four variables interact dynamically:

- The voltage (transmembrane potential), V, typically in millivolts, mV.
- The proportion of open channels, M, for the voltage-gated Ca channel that drives the rising phase of the action potential. Since M is a proportion, it ranges between 0 and 1, and has no units.
- The proportion of open channels, W, for the voltage-gated K channel that terminates the action potential. Like M, W is a proportion, so ranges between 0 and 1.
- Time, t, the independent variable, typically in milliseconds, ms.

Again, the dependent variables are functions of one another; they interact, and do so with time dependence. The rules by which they interact are translated into differential equations, as discussed below.

What is a differential equation? The only mathematical background we assume is that you have taken a calculus course sometime in the past (perhaps long ago) and remember (perhaps dimly) that the *derivative* represents instantaneous rate of change, or the slope of a graph. For example, Figure 1.1 shows several graphs of voltage, $V(t)$ versus time. Consider the detailed action potentials shown in Figure 1.1b. During the rising phase of each action potential, the slope of the graph is positive. So the derivative, $\frac{dV}{dt}$, is positive. This is just another way of saying that V is increasing or depolarizing. During the hyperpolarizing (decreasing) phase of each action potential, the graph is heading "downwards," with a negative slope, so $\frac{dV}{dt} < 0$. At the peak of each action potential, a line tangent to the graph would be horizontal, with zero slope. So $\frac{dV}{dt} = 0$ as the graph turns from increasing to decreasing. Similarly, $\frac{dV}{dt} = 0$ as the graph turns from decreasing to increasing.

(1.2.1) This is where the interactive part of the tutorial begins. This first exercise is designed to help cement the concepts of slope and derivative, and does not require any software. Choose one of the graphs in Figure 1.1 and track $\frac{dV}{dt}$ as you move along the graph. When is $\frac{dV}{dt}$ positive? When is it negative? How many times is it zero? When is $\frac{dV}{dt}$ greatest? When is it most negative? Try sketching the graph of $\frac{dV}{dt}$ below your graph of $V(t)$ (it helps to have the time axes lined up).

A *differential equation* is just an equation with a derivative in it somewhere. Equation (1.1) is a differential equation relating the rate of change

of voltage to the currents flowing through the cell membrane. The differential equation does not tell us about V directly, in the sense that it is not of the form

$$V(t) = \text{"something"}$$

But if we can measure the value of V at one *initial* moment in time, Equation (1.1) tells us how V will change, so that we can use it to predict all future values of $V(t)$. Adding up all the incremental changes in V over time is called *numerical simulation*. It can be hard to do by hand, but is a job well suited to a computer. This is one of the reasons that mathematical modeling in biology has flourished with the computer revolution of recent decades, and why this tutorial is designed to be interactive, using the numerical simulation software XPP (Ermentrout, 2012).

A word of warning: the derivative is a fundamental concept in math ematics, so has earned many names; $\frac{dV}{dt}$ ("dV by dt"), V' ("V prime"), and $\dot{V}$ ("V dot") are all equivalent in this context, and not to be confused with plain V.

The differential equation for voltage change over time. According to Kirchoff's current law, if a current I is applied across the membrane (through an electrode, say), it is balanced by the sum of the capitative and ionic currents:

$$I = C\frac{dV}{dt} + I_{\mathrm{Ca}} + I_{\mathrm{K}} + I_{\mathrm{L}}$$

If there is no applied current, then $I = 0$. Here, I_{Ca} and I_{K} denote the Ca and K currents respectively; I_{L} denotes a leak current (a voltage independent current that may or may not be selective); C denotes the capacitance, and $C\frac{dV}{dt}$ represents the capacitive current. The fact that capacitive current is proportional to how quickly voltage changes $\left(\frac{dV}{dt}\right)$ is what makes this a differential equation. Rearranging to bring the derivative to the left-hand side,

$$C\frac{dV}{dt} = I - I_{\mathrm{Ca}} - I_{\mathrm{K}} - I_{\mathrm{L}}$$

Thus,

$$C\frac{dV}{dt} = I - g_{\mathrm{Ca}}M(V - V_{\mathrm{Ca}}) - g_{\mathrm{K}}W(V - V_{\mathrm{K}}) - g_{\mathrm{L}}(V - V_{\mathrm{L}}) \tag{1.1}$$

where the ionic currents are modeled by

$$I_{\mathrm{Ca}} = g_{\mathrm{Ca}}M(V - V_{\mathrm{Ca}}) \tag{1.2}$$

$$I_{\mathrm{K}} = g_{\mathrm{K}}W(V - V_{\mathrm{K}}) \tag{1.3}$$

$$I_{\mathrm{L}} = g_{\mathrm{L}}(V - V_{\mathrm{L}}) \tag{1.4}$$

Let us walk through these equations term by term, to understand the notation, and how the ionic currents are represented. To fix ideas, consider the K current. In Equation (1.3), I_K is modeled as the product of:

- The maximal K conductance, g_K, that can be measured at any voltage (see Figure 1.2).
- The K-channel activation variable, W, which changes over time (so is written $W(t)$, or W for short). There is no K-channel inactivation in the model, so, relative to maximal conductance, $W(t)$ represents the proportion of K channels that are open at time t, and the instantaneous probability that an individual K channel is in its open state. In other words, $W(t)$ represents the normalized K conductance at time t (taking values between 0 and 1), and $g_K W(t)$ represents the absolute K conductance. Expressions for the voltage dependence and kinetics of W are formulated in Equations (1.6), (1.9), and (1.10).
- The driving force, $(V - V_K)$, on K current through the K channels. This is the difference between V of the moment and V_K, the K reversal potential. The larger the difference, the larger the driving force; and as V changes over time, the driving force changes accordingly.

Thus, Equation (1.3) is simply a mathematical translation of the fact that K current is given by K conductance multiplied by K driving force. Clear translation between the biology and the mathematics is at the heart of mathematical modeling.

The Ca and leak currents are treated similarly, with the Ca-channel activation variable denoted by M in Equation (1.2). Equation (1.4) for the leak current looks slightly different, because leak conductance is assumed to be independent of voltage, so it does not need an activation variable. Thus, the leak has constant conductance, g_L. In this tutorial, we set the conductances at $g_{Ca} = 4$, $g_K = 8$ and $g_L = 2$ (see Table 1.1).

(1.2.2) In this exercise, let us think about the impact of the K current on V, to help understand the signs in Equation (1.1). If $V > V_K$, is I_K positive or negative? It helps to remember that g_K and W are both positive. You should find that I_K is positive. So, when you check the signs in Equation (1.1), you see that the K current contributes *negatively* to $\frac{dV}{dt}$. That is, the K current promotes change in the negative direction. In the absence of other currents, what impact would this have on V? Would it increase V or decrease V? So, is the K current driving V towards V_K, or away from V_K? (Remember that we started by assuming $V > V_K$.)

(1.2.3) What happens if $V < V_K$? Explain how the K current drives V towards V_K in this case, too.

The reversal potential for a purely selective channel is equal to the Nernst equilibrium potential for the ion carrying the current. For a current representing multiple permeabilities (such as leak), the reversal potential is calculated using the Goldman–Hodgkin–Katz equation if the relative permeabilities and ionic gradients are known, or measured in voltage clamp if

the current species can be isolated (Hille 2001). In this tutorial, we set the reversal potentials at $V_{Ca} = 120$ mV, $V_K = -84$ mV, and $V_L = -60$ mV (see Table 1.1.)

Looking back at Equation (1.1), we can think of the three ionic currents competing with each other and with the applied current, each trying to drive V to its own reversal potential as in Exercises 1.2.2 and 1.2.3. Over the course of an action potential, the different voltage dependence of Ca- and K-channel gating changes the relative sizes of M and W, allowing different terms in Equation (1.1) to dominate. When the Ca term dominates, V is driven toward the high Ca reversal potential and the cell depolarizes. And when the K term dominates, V is driven back down toward the low K reversal potential and the cell hyperpolarizes (see Figure 1.4a).

The voltage dependence of steady-state conductance. K-channel activation, W, is assumed to have kinetics and voltage dependence. Both aspects are measured using the voltage clamp, as illustrated in Figure 1.2. In these experiments, the voltage is stepped instantaneously to each of a series of test voltages and held there, while the current reaches a new steady state (Figure 1.2a). Arrival at the steady state is not instantaneous, but defines the kinetics of channel activation, which is itself voltage dependent (Figure 1.2d). We return to the kinetics presently.

The amount of current at the steady state for a test voltage reflects the conformational stability of open states of the K channel; the greater the stability, the more channels open and the greater the conductance. To characterize the voltage dependence of steady-state conductance, the steady-state values of current are first plotted against test voltage to give the current–voltage (I–V) plot (Figure 1.2e). Since the measured current is assumed to be the product of driving force and conductance, the current is divided by the driving force to give the conductance–voltage (G–V) plot (Figure 1.2f). To estimate the maximal conductance, g_K, the G–V curve is fit with a Boltzmann function (Figure 1.2f), then g_K is given by the maximal value, or upper asymptote, of the Boltzmann curve. The Boltzmann function is then normalized (divided) by g_K to yield the proportion, $W_\infty(V)$, of (activatable) channels that are open at the steady state, as a function of V.

Equations (1.5) and (1.6) define the steady-state open probabilities, $M_{\infty(V)}$ and $W_{\infty(V)}$, for the Ca and K channels, respectively, in our Morris–Lecar model (see Figure 1.3b):

$$M_\infty(V) = \frac{1}{1 + e^{-2(V-V_1)/V_2}} = 0.5\left(1 + \tanh\left(\frac{V - V_1}{V_2}\right)\right) \tag{1.5}$$

$$W_\infty(V) = \frac{1}{1 + e^{-2(V-V_3)/V_4}} = 0.5\left(1 + \tanh\left(\frac{V - V_3}{V_4}\right)\right) \tag{1.6}$$

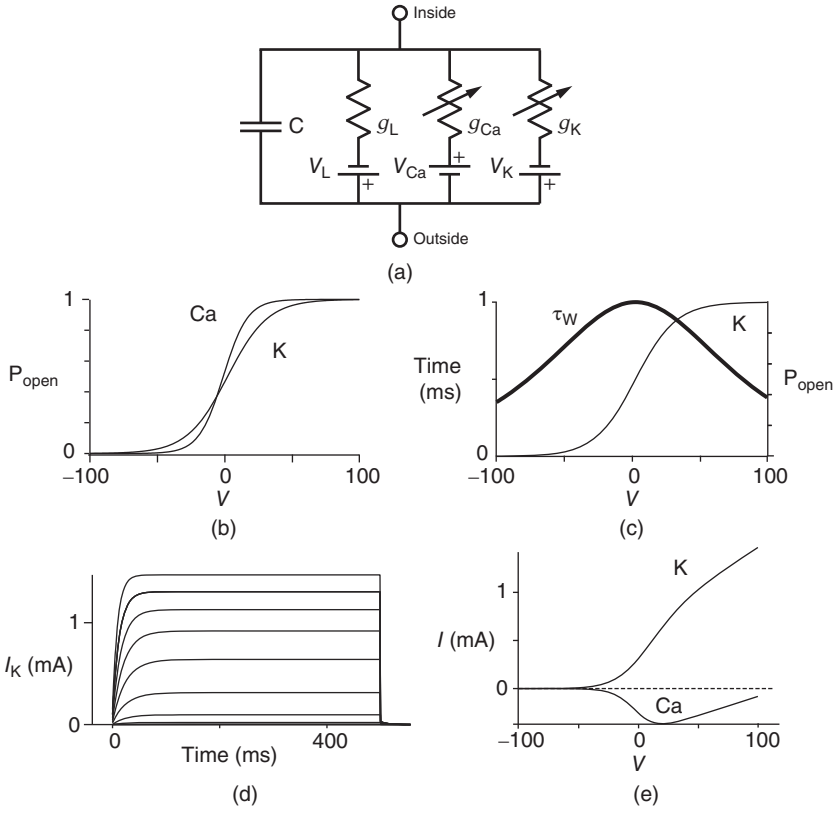

Figure 1.3 Morris–Lecar model. (a) Equivalent electrical circuit representation of the Morris–Lecar model cell. Membrane capacitance is in parallel with selective conductances and batteries (representing driving forces arising from ionic gradients). Arrows indicate variation (with voltage) for Ca and K conductance. (b) Normalized G–V curves, W_∞ and M_∞, assumed for model K and Ca conductances, respectively. (c) The kinetics of voltage-dependent activation of K channels is also voltage dependent, with the normalized time constant, τ_W, assumed to peak (i.e., channel gating slowest) at the midpoint of the G–V curve, where channel conformational preference is weakest. (d) Simulated voltage clamped K currents at 20 mV increments up to V=100 mV. Voltage clamp simulated in XPP by removing the equation for dV/dt and, instead, setting V as a fixed parameter. (e) Model I–V plots for K and Ca currents. Different reversal potentials for the two conductances ($V_K = -84, V_{Ca} = 120$ mV) make the current traces look very different, despite similar activation functions in (b). (b)–(e) Use Hopf parameter set.

In the next exercises, we will graph $W_\infty(V)$ to cement intuition for the role of V_3 and V_4. $M_\infty(V)$ is similar. In Exercise 1.2.7, we will confirm that the two different forms of the equations are, indeed, equal. The exercises are written with the online graphing calculator *Desmos* in mind, but any graphing calculator will do. We choose Desmos because it is fun to work with, and for the ease of setting up sliders to explore the way parameters

shape the graph. See Table 1.1 for the values of V_1, V_2, V_3, and V_4 used in later sections of this tutorial.

(1.2.4) Open Desmos in a browser (www.desmos.com). You enter functions in the panel on the left, and watch them appear on the axes on the right. For example, click on the left panel, and type in $y = e^x$. You should see the familiar exponential function appear. Now click on the next box on the left, and enter $y = e^{(x-c)}$. Click on the "button" to accept the offer to add a slider for c. Slide the value of c (by hand, or by clicking the "play" arrow) and watch your graph shift to the left or right accordingly. Now, try $y = d + e^{(x-c)}$. You can add a new slider for d. What is the effect of sliding d? Notice how the old c slider now works for both the functions. You can temporarily hide a graph by clicking on the colored circle next to its equation, or permanently erase it by clicking on its gray X. There is also an edit button to explore.

(1.2.5) As we have seen, Desmos uses x and y for variables, and single letters for other parameters. So, to graph $W_\infty(V)$, you will need to re-write Equation (1.6) with x playing the role of V, y playing the role of W_∞, a playing the role of V_3 and b playing the role of V_4. In other words, working with the Boltzmann form of Equation (1.6) first, enter

$$y = \frac{1}{1 + e^{(-2(x-a)/b)}} \tag{1.7}$$

(being careful with your parentheses!), and accept the sliders for a and b. You should see a typical (normalized) G–V curve ranging between 0 and 1, as shown in Figures 1.2f, 1.3b, and 1.3c. Slide a and b to see what role they play in shaping the curve. You can change the limits of the sliders if you like. For example, click on the lower limit of b and set it to zero, to keep b positive.

(1.2.6) Translating back to the language of Equation (1.6), confirm that V_3 is the half-activation voltage of W_∞, and V_4 determines the "spread" of W_∞. As V_4 increases, the spread increases. In other words, as V_4 increases, the slope at half-activation decreases. In fact, differentiating Equation (1.6) at $V = V_3$ shows that the slope at half-activation is given by $\frac{1}{2V_4}$. Confirm this with Desmos, by graphing the line $y = \frac{1}{2} + \frac{1}{2b}$ (which has slope $\frac{1}{2b}$) together with Equation (1.7), setting $a = 0$, and sliding b.

(1.2.7) Use Desmos to plot

$$y = 0.5\left(1 + \tanh\left(\frac{x-a}{b}\right)\right) \tag{1.8}$$

and confirm that this second form of Equation (1.6) is equivalent to the first. In other words, it has exactly the same graph. This second form is also commonly used, and you will see it in the XPP code provided. If you are unfamiliar with the hyperbolic tangent function, $\tanh x$, develop your intuition by building up the graph of Equation (1.8) in parts. First

graph $y = \tanh x$, then $y = \tanh(x - a)$, etc. (Recall that the more familiar $\sin x, \cos x$, and $\tan x$ are defined using a point on the unit circle $x^2 + y^2 = 1$. The hyperbolic functions $\sinh x$, $\cosh x$, and $\tanh x$ have analogous definitions using a point on the hyperbola $x^2 - y^2 = 1$.)

Voltage-dependent kinetics of voltage gating. Now we return to the kinetics of K-channel gating, governing the rate of approach to the steady state. The channels are trying to reach the steady state for conductance at a particular voltage, but during the process the voltage is typically changing. As a result, the channels are always playing catch-up. Moreover, the rate at which the channels respond to voltage is itself a function of voltage. These kinetics are modeled by the differential equation

$$\frac{dW}{dt} = \frac{\phi}{\tau_W(V)}(W_\infty(V) - W) \tag{1.9}$$

Here, ϕ and $\tau_W(V)$ are both positive, and together define the time scale (or time constant) of K kinetics. The voltage dependence of the time scale is captured by the equation for $\tau_W(V)$

$$\tau_W(V) = \frac{1}{\cosh((V - V_3)/2V_4)} \tag{1.10}$$

See Figure 1.3c. We will develop intuition for Equations (1.9) and (1.10) in the following exercises. See Table 1.1 for the values of ϕ, V_3, and V_4 used in later sections of this tutorial.

(1.2.8) First let us focus on the $(W_\infty(V) - W)$ term in Equation (1.9). It is reminiscent of the $(V - V_K)$ term in Equation (1.3), and can be analyzed in a similar way. Recall that V and W change over time. So, at a given time t, V and W will have values $V(t)$ and $W(t)$. What happens if, at time t, $W(t) > W_\infty(V(t))$? Will W increase or decrease in the next increment of time? Remember that ϕ and $\tau_W(V)$ are both positive. So, if you keep track of the signs, you should find that if $W(t) > W_\infty(V(t))$, then $dW/dt < 0$, so W is driven down, toward $W_\infty(V(t))$.

(1.2.9) What happens if $W(t) < W_\infty(V(t))$? Explain how the conductance is driven towards steady state in this case, too. As time marches on, V changes. So the voltage-dependent steady-state conductance, $W_\infty(V)$, also changes. Thus, the $(W_\infty(V) - W)$ term in Equation (1.9) ensures that W adjusts course accordingly, in its tireless game of catch-up.

(1.2.10) Now, let us focus on $\tau_W(V)$ to prepare us for understanding its role in Equation (1.9). Use Desmos to graph $\tau_W(V)$, as shown in Figure 1.3c. Recall that you will need to rewrite the equation for $\tau_W(V)$ with x playing the role of V, y playing the role of τ_W, and single letters playing the role of V_3 and V_4. For example, you could graph

$$y = \frac{1}{\cosh((x - a)/2b)} \tag{1.11}$$